Influences of lamin A levels on induction of pluripotent stem cells

Bingfeng Zuo[1,2,*], Jiao Yang[1,*], Fang Wang[1], Lei Wang[1], Yu Yin[1], Jiameng Dan[1], Na Liu[1] and Lin Liu[1,‡]

[1]State Key Laboratory of Medicinal Chemical Biology, Department of Genetics and Cell Biology, College of Life Sciences, Nankai University, Tianjin 300071, China
[2]Tianjin-Oxford Joint Laboratory of Gene Therapy, Tianjin Research Centre of Basic Medical Science, Tianjin Medical University, Tianjin 300070, China

*These authors contributed equally to this work
‡Author for correspondence (liulin@nankai.edu.cn; liutelom@yahoo.com)

Biology Open 1, 1118–1127
doi: 10.1242/bio.20121586
Received 7th April 2012
Accepted 8th August 2012

Summary

Lamin A is an inner nuclear membrane protein that maintains nuclear structure integrity, is involved in transcription, DNA damage response and genomic stability, and also links to cell differentiation, senescence, premature aging and associated diseases. Induced pluripotent stem (iPS) cells have been successfully generated from various types of cells and used to model human diseases. It remains unclear whether levels of lamin A influence reprogramming of somatic cells to pluripotent states during iPS induction. Consistently, lamin A is expressed more in differentiated than in relatively undifferentiated somatic cells, and increases in expression levels with age. Somatic cells with various expression levels of lamin A differ in their dynamics and efficiency during iPS cell induction. Cells with higher levels of lamin A show slower reprogramming and decreased efficiency to iPS cells. Furthermore, depletion of lamin A by transient shRNA accelerates iPS cell induction from fibroblasts. Reduced levels of lamin A are associated with increased expression of pluripotent genes Oct4 and Nanog, and telomerase genes Tert and Terc. On the contrary, overexpression of lamin A retards somatic cell reprogramming to iPS-like colony formation. Our data suggest that levels of lamin A influence reprogramming of somatic cells to pluripotent stem cells and that artificial silencing of lamin A facilitates iPS cell induction. These findings may have implications in enhancing rejuvenation of senescent or older cells by iPS technology and manipulating lamin A levels.

© 2012. Published by The Company of Biologists Ltd. This is an Open Access article distributed under the terms of the Creative Commons Attribution Non-Commercial Share Alike License (http://creativecommons.org/licenses/by-nc-sa/3.0).

Key words: Lamin A, Reprogramming, Pluripotency, iPS, ES, Differentiation

Introduction

Lamin A encoded by the LMNA gene is a major nuclear architectural protein important for maintaining nuclear membrane inner structure integrity and function (Dechat et al., 2008). Lamin A is involved in regulation of gene expression in health and disease through interplay with cell cycle progression, DNA replication, signal transduction pathways, transcription factors, chromatin-associated proteins and tissue homeostasis (Andrés and González, 2009; Broers et al., 2006; Naetar and Foisner, 2009). Dysfunction of lamin A triggers DNA damage response, cellular senescence or apoptosis (Bridger and Kill, 2004; Lees-Miller, 2006; Musich and Zou, 2009). LMNA mutations cause a variety of human diseases termed laminopathies, including progeroid syndromes and premature-ageing disorders, e.g. Hutchinson-Gilford Progeria Syndrome (HGPS) (Andrés and González, 2009; Csoka et al., 2004; Decker et al., 2009; Naetar and Foisner, 2009; Scaffidi and Misteli, 2008). A-type lamins are regarded as intrinsic modulators of ageing within adult stem cells and their niches that are essential for survival to old age (Pekovic and Hutchison, 2008). Increased expression of HGPS truncated lamin A transcript accelerates a subset of the pathological changes that contribute to aging processes (Burtner and Kennedy, 2010; Rodriguez et al., 2009). Notably, mice carrying lamin A mutation also display defects consistent with HGPS (Mounkes et al., 2003).

Lamin A also may control the onset of aging-associated decline in normal fibroblasts (Kudlow and Kennedy, 2006). Increased levels of wild-type lamin A in normal human cells result in decreased replicative lifespan and nuclear membrane alterations that lead to apoptotic cell death and senescence in a manner that is strongly reminiscent of the phenotype shown by HGPS cells and that are also observed in cells from old-age individuals (Candelario et al., 2008), suggesting that the elevated levels of lamin A are associated with aging. Modeling of premature ageing syndromes by generation of induced pluripotent stem (iPS) cells from HGPS patients (Ho et al., 2011; Liu et al., 2011a; Liu et al., 2011b; Zhang et al., 2011), and from patients with dyskeratosis congenita (Agarwal and Daley, 2011; Agarwal et al., 2010), could provide *in vitro* model to understand the mechanisms of development of diseases and aging processes and help developing novel therapeutic drugs for interference of diseases.

During development, A-type lamins do not appear until midway through embryonic development, suggesting that these proteins may be involved in the regulation of terminal differentiation (Röber et al., 1989). In adult tissues, expression of lamin A differs

at different stages of cell differentiation, and plays critical roles in transcriptional activation of genes important for differentiation (Peric-Hupkes et al., 2010; Stewart and Burke, 1987; Takamori et al., 2007). Moreover, mice lacking A-type lamins develop to term without overt abnormalities (Sullivan et al., 1999), indicating that lamin A deficiency itself does not negatively affect embryonic development and differentiation during fetal development. However, A-type lamins are required for postnatal growth and the maintenance of quiescence and differentiation (Pekovic and Hutchison, 2008; Sullivan et al., 1999). Pluripotent embryonic stem (ES) cells generated from preimplantation embryos maintain unlimited self-renewal and undifferentiated states, yet do not express lamin A in the nuclear envelope (Bru et al., 2008; Butler et al., 2009; Constantinescu et al., 2006). Absence of lamin A in ES cells and strong expression of lamin A in the nuclear envelope of somatic cells may allow distinguishing pluripotent stem cells from differentiated cells.

While stemness facilitates reprogramming, as shown by more efficient reprogramming of progenitor stem cells to iPS cells than of differentiated cells (Eminli et al., 2009), cell senescence impairs reprogramming to pluripotency in iPS induction (Banito et al., 2009). Recently, iPS cells have been generated from HGPS patients (Ho et al., 2011; Liu et al., 2011a; Liu et al., 2011b; Zhang et al., 2011). Whether levels of lamin A in somatic cells influence reprogramming efficiency of iPS induction has not been directly addressed. Also, it remains unclear whether mouse cells show efficient reprogramming of lamin A during iPS induction to become silenced, like ES cells. We tested the hypothesis that levels of lamin A in somatic cells influence reprogramming and pluripotency. Minimizing levels of lamin A might enhance iPS cell induction.

Results

Expression of lamin A in various mouse cell types

Lamin A was highly expressed in the nuclear membrane of adult mouse tail-tip fibroblasts (TTF) that showed absent Oct4 expression, whereas Oct4 was specifically expressed in the nuclei of ES cells that showed no visible expression of lamin A in the nuclear membrane (Fig. 1A). Lamin A also may control the onset of aging-associated decline in normal human fibroblasts, and increased levels of wild-type lamin A lead to apoptotic cell death and senescence (Candelario et al., 2008; Kudlow and Kennedy, 2006). Levels of lamin A also may link to differentiation of stem cells (Pekovic and Hutchison, 2008; Sullivan et al., 1999). We further assessed the lamin A expression in various cell types from various ages of C57BL/6 mice, and also compared with that of ES cells served as negative controls. J1 ES was used as controls because they were maintained as undifferentiated state without mouse embryonic fibroblasts (MEF) feeders to eliminate the feeder cell contamination that complicates lamin A quantification. MEFs as feeders showed high expression of lamin A. Consistent with immunostaining data, lamin A was at minimal or undetectable level in ES cells, whereas lamin A was at high levels in somatic cells (Fig. 1B,C). Moreover, levels of lamin A were higher in differentiated adult somatic cells TTF from older mice (8 months of age) than in TTF from younger mice and at earlier passages. MEFs showed lower levels of lamin A than those of TTF, and mesenchymal stem cells (MSCs) at P1 expressed much lower levels of lamin A than other somatic cells (Fig. 1C). The mRNA levels of lamin A generally corresponded to the protein levels by Western blot analysis (Fig. 1D). By relative quantification using β-actin as internal loading reference and Bio-rad software, the protein levels of

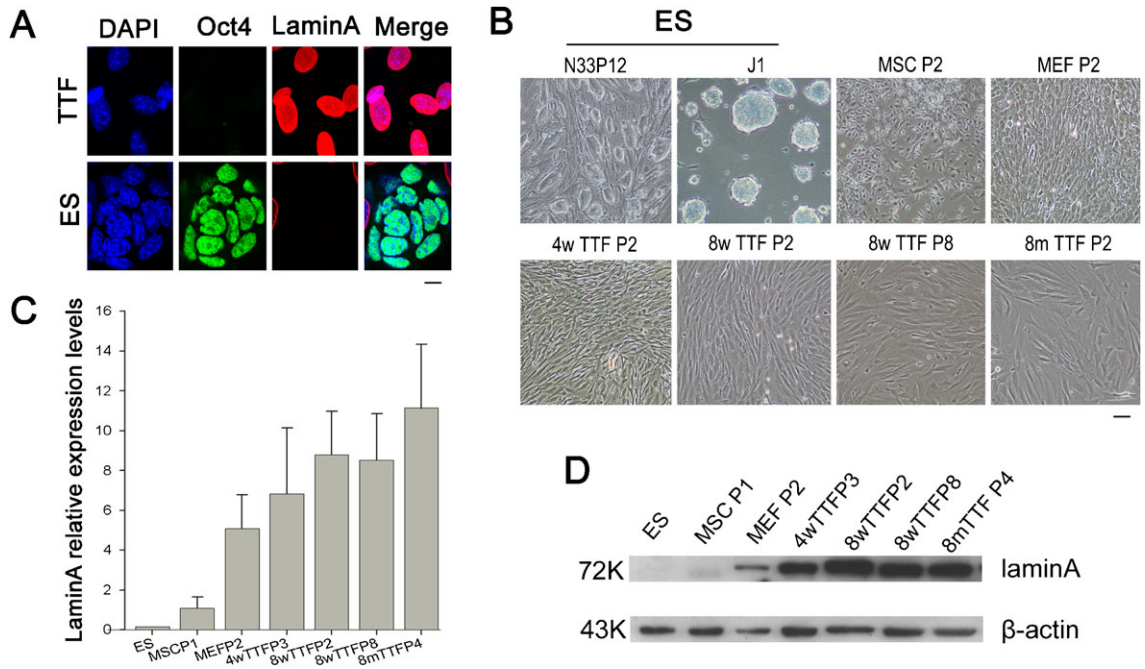

Fig. 1. Relative expression levels of lamin A in various types of mouse cells. (**A**) Comparison of the localization and relative expression levels of ES cell markers Oct4 (green) and lamin A (red) between mouse tail-tip fibroblast (TTF) and normal ES cells by immunofluorescence staining and microscopy. Nuclei stained with DAPI (blue). Bar=5 µm. (**B**) Micrographic morphology of various mouse cell types cultured at different passages (P). Bar=50 µm. (**C**) Relative expression of lamin A by quantitative real-time PCR analysis. Mouse J1 ES cells without feeder cells served as negative controls. (**D**) Western blotting analysis showing relative protein levels of lamin A in mouse somatic cells, compared to mouse J1 ES cells. β-actin served as loading control. MSC, mesenchymal stem cells from 5 week old C57BL/6 mouse; N33, ES cells from C57BL/6; MEF, mouse embryonic fibroblasts. w, weeks of mouse age; m, months of mouse age.

lamin A in MEFs were higher than those of MSCs and lower than those of TTFs at early passages. Together, aging somatic cells express higher levels of lamin A, whereas younger cells at early passages show lower levels of lamin A, suggesting that reduced levels of lamin A are associated with the youth and stemness.

Levels of lamin A influence reprogramming of iPS cell induction

We sought to test whether expression levels of lamin A influence reprogramming efficiency of fibroblasts to iPS cells. We have shown that MSCs generated iPS cells with high efficiency (Fan et al., 2011). Here, MEFs and TTF from young and older mice isolated from C57BL/6 with three different expression levels of lamin A were chosen for iPS induction by transfection of Yamanaka factors (Okita et al., 2007) (see Materials and Methods). During iPS induction, cells began to aggregate by day 3, and MEFs formed colony aggregates as early as day 6, but TTF from 8 month old mice did not (Fig. 2A), suggesting earlier reprogramming of MEFs in contrast to slower processes of iPS-like primary clone formation from TTF particularly from older mice. Consistently, MEFs gave rise to alkaline phosphatase (AP) positive iPS-like colonies at higher frequency than did TTFs, and TTF from 4 week old mice generated more iPS-like clones than did TTF from 8 month old mice (Fig. 2B). These data suggest that cells with elevated expression levels of lamin A show slower processes and reduced efficiency in iPS induction. We recently examined dynamics of expression of pluripotent genes Nanog, Oct4 and telomerase genes Tert and Terc during induction of iPS cells from TTFs and found that these genes gradually activated, but Terc activated earlier than endogenous Oct4 and Nanog (Wang et al., 2012). Also, MEFs showed increased expression of endogenous pluripotent genes Nanog and Oct4 and telomerase genes, particularly Terc during iPS induction (Fig. 2C). Under the same culture and induction condition, TTFs from 8 week old mice showed dynamic expression of Nanog, Oct4, Tert and Terc during reprogramming. Interestingly, the expression of these genes also increased but to less extent during iPS induction from TTFs, compare to those of MEFs. We speculate that higher levels of lamin A in TTFs may negatively affect expression of pluripotent genes, and slow down progress of iPS induction.

Depletion of lamin A facilitates iPS cell induction

We further tested whether reduced levels of lamin A by RNA interference directly influence efficiency of iPS induction. Levels of lamin A in C57BL/6 MEFs was effectively reduced to about 20% of the control lamin A by retrovirus-mediated lamin A shRNA interference (pSIREN-RetroQ-laminA-shRNA) in two independent experiments (Fig. 3A–D). MEFs exhibited normal morphology 48 h after RNA interference (Fig. 3A). Efficient knockdown of lamin A at 48 h by lamin A shRNA was characterized by immunofluorescence microscopy (Fig. 3B), and verified by quantitative PCR and western blot analysis (Fig. 3C,D). Lamin A-RNAi MEFs showed lower levels of lamin A than those of control-RNAi MEFs.

MEFs tended to undergo cell senescence after only a few passages in culture, such that we were unable to obtain stable MEF lines with depleted lamin A by RNAi for iPS cell induction. Thus, MEFs with reduced levels of lamin A at 48 h following shRNA of lamin A were used for induction of iPS cells, and compared directly with those of control shRNA. Dynamic changes in morphology of MEFs occurred and Nanog GFP expressed also earlier in lamin A knockdown MEFs following transfection of Yamanaka factors, compared to shRNA controls. Compact iPS-like colonies with clear boundary formed by day 12 in the lamin A knockdown MEFs, in contrast to loosened cell

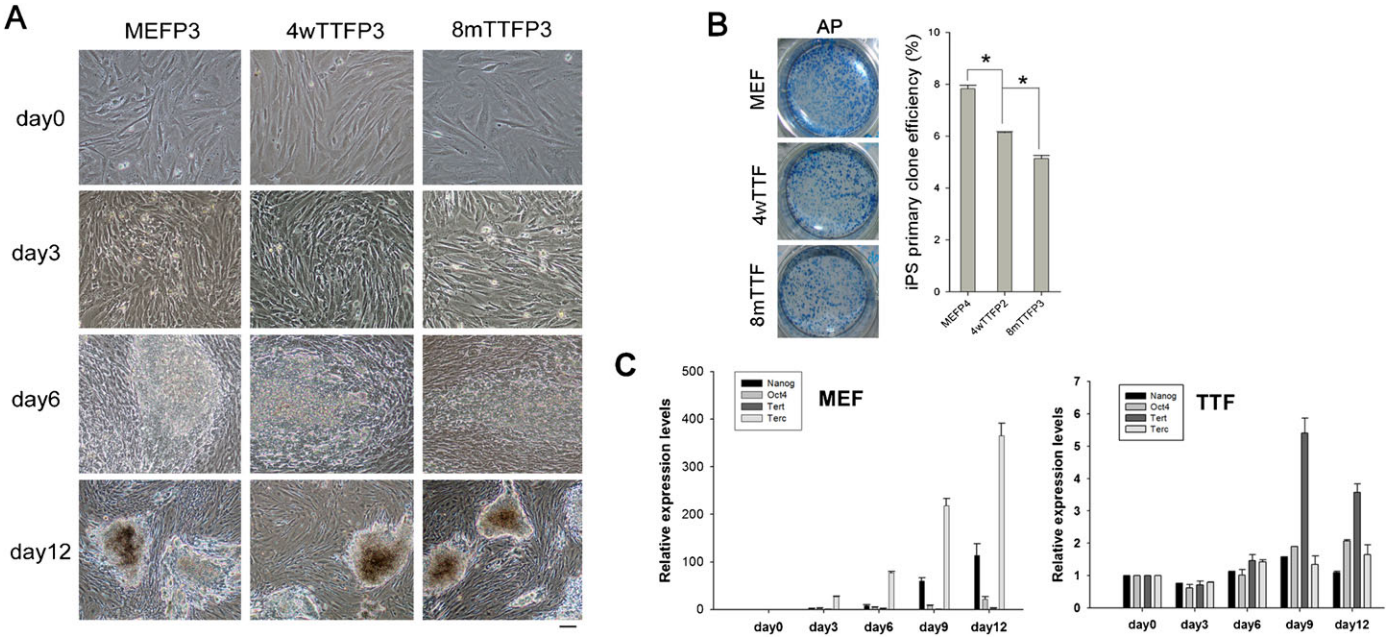

Fig. 2. Reprogramming efficiency of fibroblasts during induction of iPS cells. (**A**) Morphology of three somatic cell types isolated from C57BL/6 with different lamin A expression levels during induction of iPS and their primary iPS-like clones following transfection of four Yamanaka factors. Bar=50 µm. (**B**) Efficiency of iPS primary clones on day 11 estimated by alkaline phosphatase (AP) activity assay, based on cells (1×10^4) per well at day 6. Bars=mean ± s.e.m (n=3); *, $P<0.05$. (**C**) Expression of endogenous pluripotent genes Nanog and Oct4 and telomerase genes (Tert and Terc) during induction of iPS cells from C57BL/6 MEF and TTF from 8 week old mice. Pre-transfected cells (day 0) served as controls. w, weeks of mouse age; m, months of mouse age.

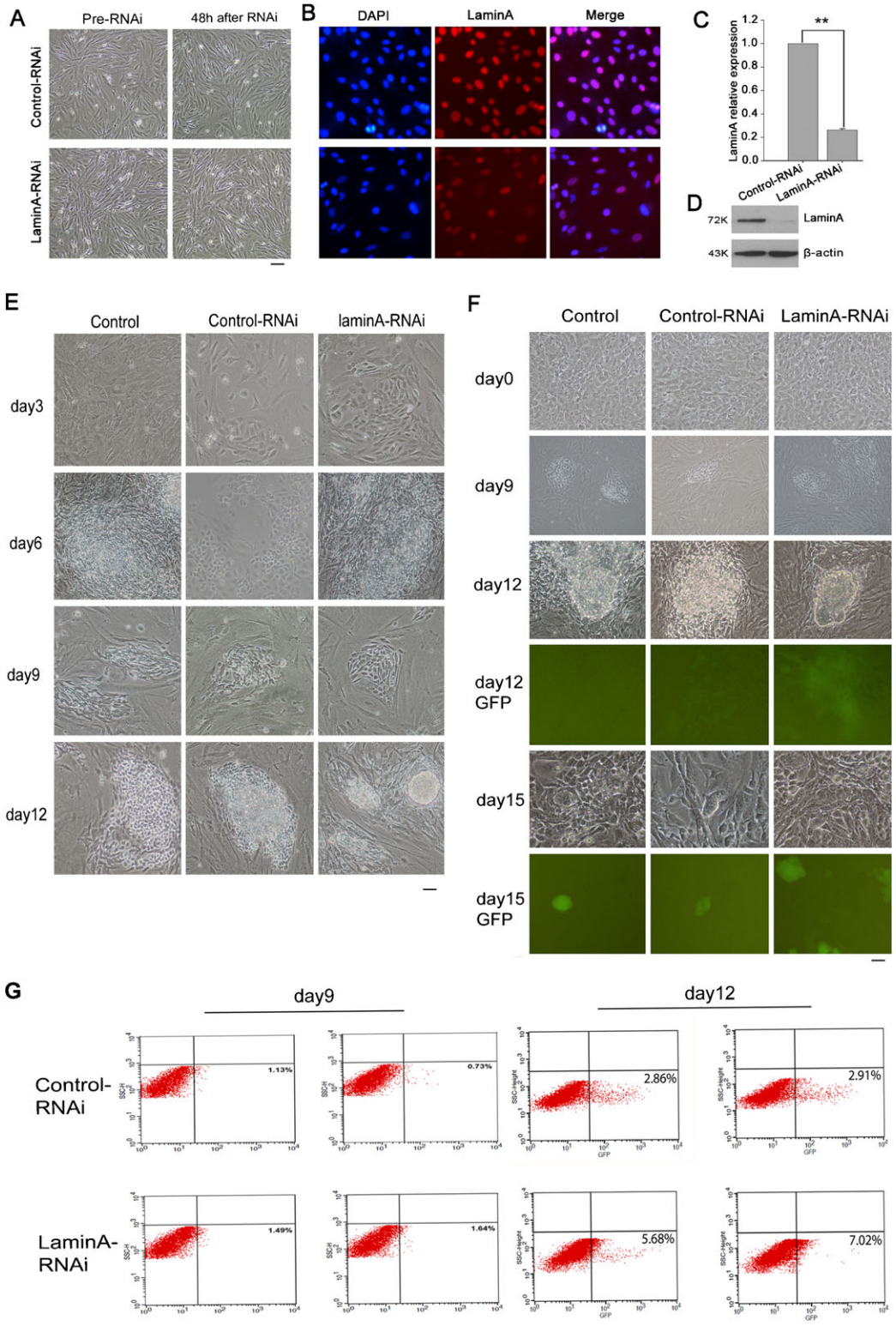

Fig. 3. Lamin A suppression facilitates iPS cell generation. (**A–D**) Efficient knockdown of lamin A in C57BL/6 MEFs by shRNA interference. (A) Morphology of MEF prior to retrovirus-mediated RNA interference or at 48 h after RNA interference. Bar=25 μm. (B) Immunofluorescence of lamin A 48 h following RNAi knockdown. (C) Relative expression of lamin A by real-time PCR analysis. **P<0.01 (n=4). (D) Levels of lamin A protein by Western blotting analysis of MEFs at 48 h after retrovirus-mediated RNA interference. (**E**) Morphological dynamics of MEF cells during reprogramming to iPS induction. The control group was MEFs that were transfected with the four Yamanaka factors virus directly; the control-RNAi MEFs were transfected with control-shRNA virus two days prior to transfection of the four factors; the laminA-RNAi MEFs were transfected with laminA-shRNA virus two days prior to transfection of the four factors. Bar=50 μm. (**F**) Morphology and green fluorescence during reprogramming of Nanog-GFP transgenic mouse MEF cells. GFP green fluorescence appeared in the laminA-RNAi MEFs at day 12, but minimal in other two control groups. Bar=50 μm. (**G**) Representative plots by FACS and the percentage of events indicated in the quadrant showing expression of GFP in Nanog-GFP MEFs with control shRNA (Control-RNAi) or laminA shRNA (laminA-RNAi). Data from duplicate.

aggregates in the control MEFs (Fig. 3E). Likewise, Nanog GFP of lamin A knockdown MEFs appeared as early as day 9 and more evident at day 12, whereas control RNAi MEFs showed no obvious expression of GFP at day 12. These data show that reduced levels of lamin A by shRNA accelerate the iPS colony formation. By continuous culture without pick up of the colonies, about 3–4 fold increases in Nanog-GFP clones with brighter GFP fluorescence were found in lamin A knockdown MEFs at day 15, compared to control MEFs (Fig. 3F). Consistently, the percentage of Nanog- GFP-positive cells by flow cytometry analysis doubled from day 9 to day 12 during iPS induction following lamin A knockdown, compared to controls (Fig. 3G), indicating increased efficiency of reprogramming by RNAi for lamin A. Early formation and increased frequency of iPS-like clones by lamin A knockdown suggests that reduced levels of lamin A facilitates reprogramming processes of iPS induction.

By immunofluorescence microscopy, fewer MEFs showed expression of lamin A during reprogramming by lamin A-shRNA than those of controls (Fig. 4A). Real-time PCR analysis confirmed that expression levels of lamin A in lamin A-shRNA MEFs were much lower than those of controls during iPS induction (Fig. 4B). Expression of endogenous pluripotent genes Nanog, Oct4 and Essrb was increased in subpopulations of MEFs during iPS induction, and lamin A-shRNA MEFs showed even higher increased levels of Nanog and Essrb (about 2 fold) and Oct4 (about 3 fold) by day 12, compared to controls (Fig. 4B).

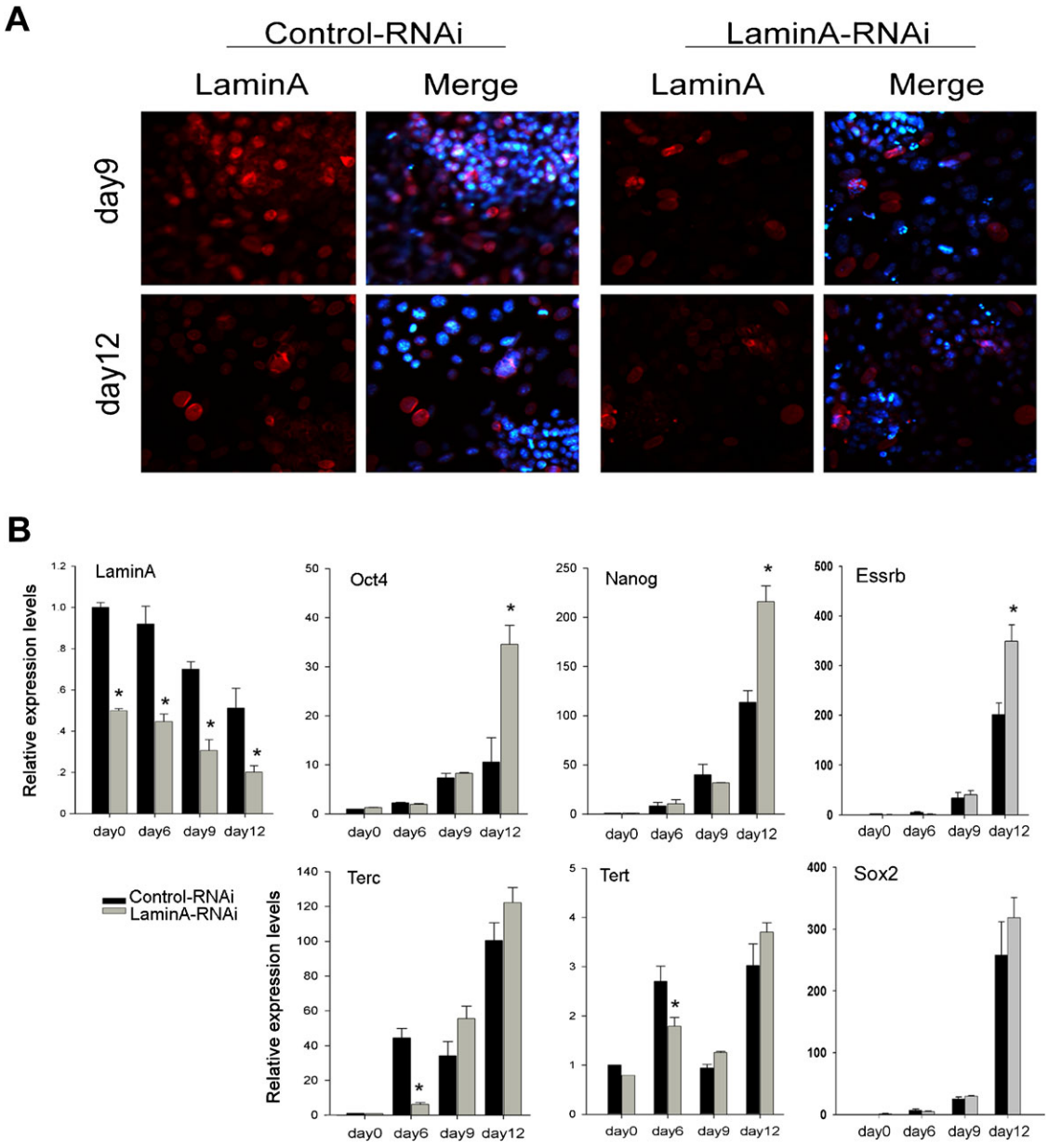

Fig. 4. Expression of lamin A and pluripotent genes during induction of iPS from MEFs by RNA interference. (**A**) Immunofluorescence micrographs showing lamin A (Red) expression during somatic cell reprogramming between Control (+4 Yamanaka factors and control shRNA) and lamin A-RNAi group (+4 Yamanaka factors and lamin A shRNA). Nuclei stained with DAPI (Blue). (**B**) Relative expression of lamin A, Nanog, Oct4, Essrb, Sox2, Tert and Terc by real-time PCR analysis during iPS induction.

The difference at day 12 may reflect a role for lamin A in expansion of iPS cells, but not the early reprogramming process *per se*. In general, expression of Tert and Terc was increased during iPS induction and these increases were not apparently affected by lamin A-shRNA. These data show that reduced levels of lamin A facilitate iPS cell production, coincided with increased expression of endogenous pluripotent genes.

Further, iPS cell lines generated from lamin A knockdown MEFs exhibited morphology typical ES cell colonies, and resembled iPS cells induced from control RNAi MEFs (Fig. 5A). Regardless of lamin A depletion, the formed iPS cells at early passage were negative for lamin A by immunostaining but positive for pluripotent markers, Oct4, Nanog and SSEA1. Like control iPS cells, Lamin A-RNAi iPS cells exhibited active and repressive histone methylation patterns shown by immunostaining of H3K4me3 and H3K9me3/H3K27me3 (Fig. 5B). It seemed, however, that the levels of H3K9me3 and H3K27me3 marks associated with gene silencing were decreased, whereas Oct4, Nanog and SSEA1 immunofluorescence increased in iPS cells after lamin A RNAi. More than 70% of lamin A-RNAi iPS cells had normal karyotype of 40 chromosomes, similar to control-RNAi iPS cells (Fig. 5C). Also, their telomere lengths estimated by T/S ratio did not differ between Lamin A-RNAi and control iPS cells (Fig. 5D). Overall, early passage iPS cells derived from lamin A-depleted MEFs show chromosome stability and express markers for pluripotency, like ES cells.

Overexpression of lamin A reduces iPS induction

Next, we tested whether overexpression of lamin A retards dynamics of reprogramming to iPS cells. Nanog-GFP MEFs overexpressing lamin A and control MEFs transfected with mock vectors were induced to iPS in KSR based induction media. During our independent experiments, we found that iPS induction in FBS based media was slower than in KSR based media (data not shown), consistent with recent report (Okada et al., 2010). The cell aggregates were visible in the control MEFs by day 6 of induction and the primary clones formed around day 10, whereas MEFs overexpressing lamin A slowly formed aggregations by day 10 (Fig. 6A,B). By day 12, ES-like primary iPS-like clones with Nanog GFP fluorescence were formed in the control MEFs. In contrast, Nanog-GFP fluorescence was not visible in iPS-like

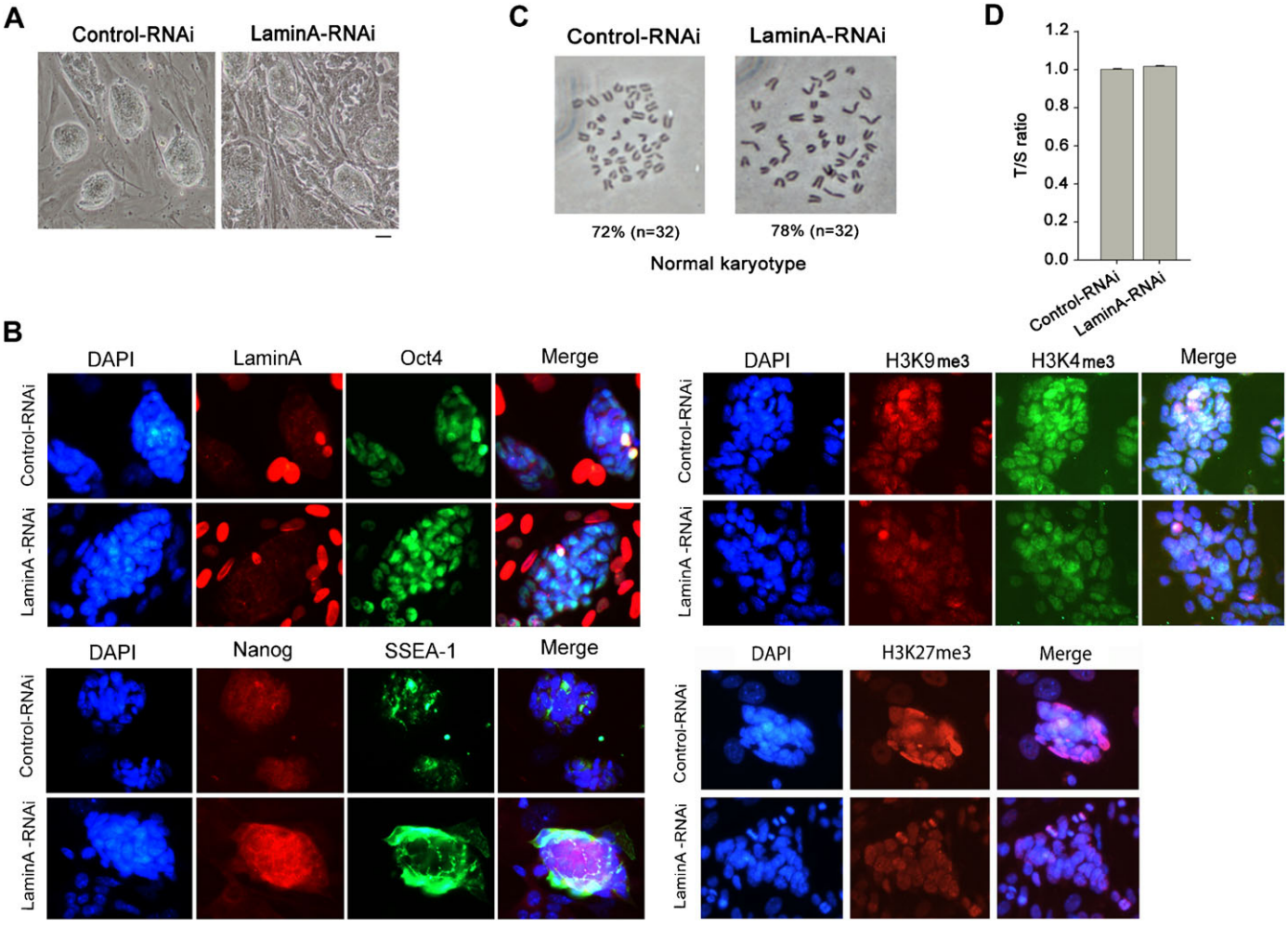

Fig. 5. Characterization of iPS cell lines generated from lamin A-RNAi MEFs. (**A**) Clonal morphology of iPS cells at passage 7 under bright field (BF) with phase contrast optics. Bar=100 μm. (**B**) Immunofluorescence staining of lamin A, Oct4, Nanog, SSEA1 and methylated histones H3K4me3/H3K9me3/H3K27me3 between control and lamin A-RNAi iPS cell lines. Nuclei stained with DAPI (blue). (**C**) Representative karyotype of normal iPS and lamin A-RNAi iPS at passage 7. (**D**) Relative telomere length as indicated by T/S ratio measured by real-time PCR method.

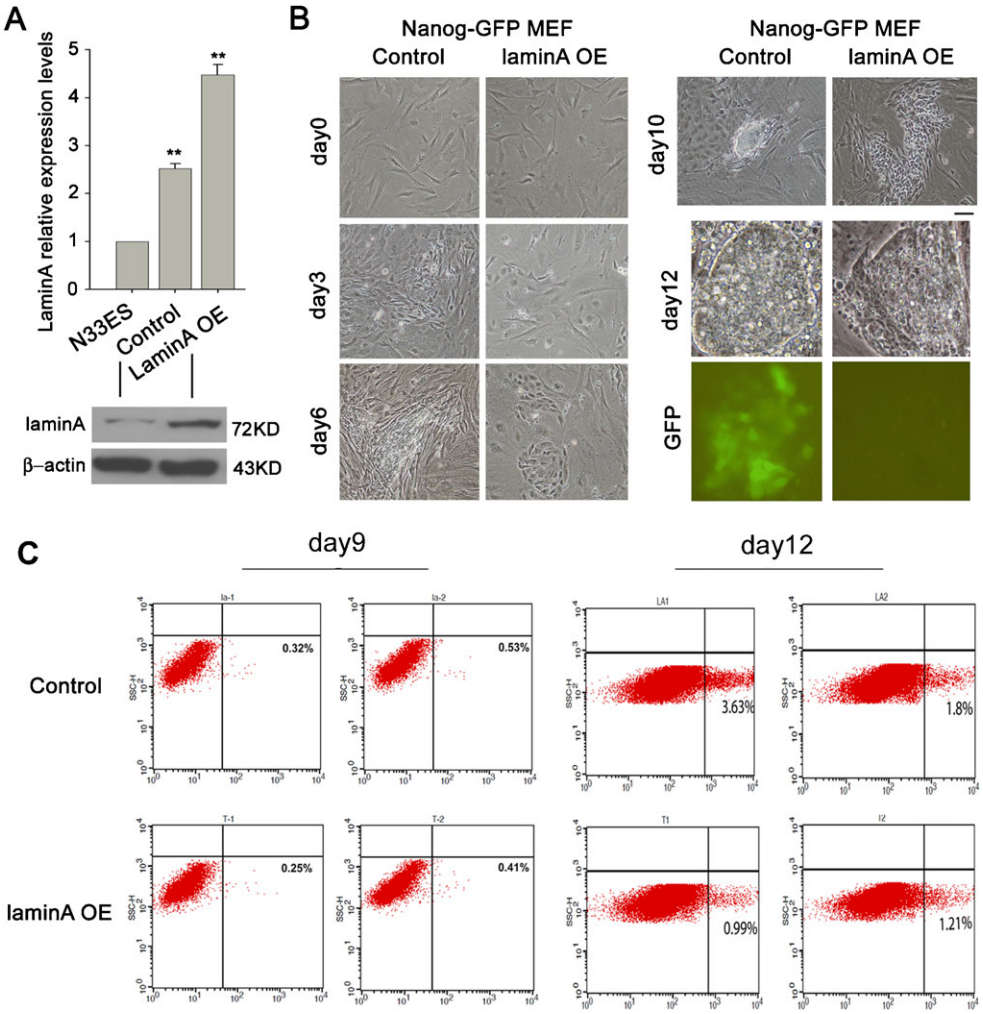

Fig. 6. Overexpression of lamin A decreases reprogramming and induction of iPS cells. (**A**) Expression by qPCR of lamin A is significantly increased in Nanog-GFP MEFs from C57BL/6 mice 48 h following overexpression (OE) of lamin A. N33 ES cells also from C57BL/6 background served as controls, and relative expression value arbitrarily designated as 1. Bottom panel indicates verification by Western blot analysis. Low levels of lamin A were detected in N33ES cells, likely due to contamination of feeder MEFs, in contrast to J1ES cells maintained in the absence of feeders (Fig. 1). (**B**) Dynamics of iPS cell induction in KSR based induction media from Nanog-GFP MEFs and Nanog-GFP MEFs overexpressing lamin A. Bar=50 µm. (**C**) Representative plots by FACS analysis and the percentage of events indicated in each quadrant showing expression of GFP in normal Nanog-GFP MEFs with only vector (Control) and Nanog-GFP MEFs with laminA overexpression (laminA-OE) at day 9 and day 12 during reprogramming. Data from duplicate.

primary clones that also formed in lamin A overexpression MEFs. Consistently, the percentage of Nanog- GFP-positive cells by flow cytometry analysis was decreased 2–3 fold by day 12 during iPS induction in lamin A overexpression MEFs, compared to controls (Fig. 6C), showing that lamin A overexpression indeed reduces reprogramming efficiency. These data suggest that cells with higher levels of lamin A could be induced to form iPS-like clones but at lower pace and quality.

Discussion

Lamin A expression differs in somatic cells versus pluripotent stem (iPS/ES) cells

Expression levels of lamin A in ES or iPS cells are very low, and these cells do not show lamin A immunostaining in the nuclear membrane, whereas somatic cells (mouse fetal fibroblasts and adult fibroblasts) express high levels of lamin A, and the levels of lamin A increase with cell senescence during passages and with organism age, consistent with previous findings (Candelario et al., 2008; Kudlow and Kennedy, 2006). MSCs show reduced expression of lamin A but somatic fibroblasts from older mice increased levels of lamin A. This is consistent with a previous report that lamins A/C are not or only marginally present in the somatic stem cells or progenitor stem cells (Takamori et al., 2007). Misregulation of lamin A of adult stem cells is associated with accelerated ageing (Scaffidi and Misteli, 2008). Low levels of lamin A are associated with higher potential of proliferation and differentiation capacity. High expression of lamin A in somatic cells is reduced to minimal levels during reprogramming to iPS cells. Consistently, lamin A/C found only in differentiated cells is also removed from their nuclei by exposure of the somatic cells to ES cell extracts, and reprogramming of gene expression for pluripotency is induced (Bru et al., 2008). Differential expression of lamin A in somatic cells versus pluripotent stem cells might suggest function of lamin A in differentiated cells quite different from that of iPS/ES cells.

High levels of lamin A in TTF from older mice lead to slower dynamics of reprogramming and reduced rates of iPS-like colony formation. Lamin A reduction by shRNA enhances early reprogramming of iPS cell induction.

Lamin A limits pluripotency in association with induction of differentiation

Absence of A-type lamin expression is identified as a novel marker for undifferentiated ES cells (Constantinescu et al., 2006). Increased levels of lamin A and reduced expression of pluripotent genes are essential for ES cell differentiation. By contrast, depletion of lamin A by RNAi leads to earlier activation of Nanog and Oct4, facilitating reprogramming. Lamin A might directly inhibit activation of pluripotent genes and telomerase genes or indirectly influence their expression by Wnt signaling or

other pathways. Critical amount of Oct4 and Nanog is required to sustain stem-cell self-renewal and undifferentiated states; either high or low expression of the genes leads to differentiation of ES cells (Chambers et al., 2007; Niwa et al., 2000). It is likely that lamin A negatively regulates expression of pluripotent genes, activating expression of genes for differentiation, but this speculation requires further experimentation to validate.

Indeed, high resolution maps of genome-nuclear lamina interactions reveal that expression of pluripotent genes Oct4, Nanog and several others depends on their spatial distribution relative to nuclear lamina (Peric-Hupkes et al., 2010). Nuclear lamina seems to repress their activation when they locate closely to the lamina as seen in differentiated cells, while this repression is removed when these genes move away from nuclear lamina presumably in undifferentiated ES cells, consistent with high levels of Oct4 and Nanog in ES cells. Depletion of lamin A in the nuclear lamina of ES cells might link to the desuppression of Oct4 and Nanog and other genes associated with stemness. Mechanisms underlying the dynamics and their relationships of lamin A and pluripotent genes and telomerase genes remain further investigation.

Lamin A depletion does not shorten telomeres in pluripotent stem cells

Lamin A deficiency abrogates telomere integrity and leads to telomere shortening in differentiated somatic cells (De Vos et al., 2010; Gonzalez-Suarez et al., 2009; Uhlírová et al., 2010), in association with defective membrane structure (Shimi et al., 2008). Also, fibroblasts from premature aging HGPS patients exhibit shorter telomeres than those of age-matched controls (Decker et al., 2009). We were concerned about whether telomeres were shortened by lamin A depletion during iPS cell induction. Intriguingly, like ES cells, iPS cells express no or minimal lamin A which is invisible in the nuclear envelope, yet they do not show shortened, but instead elongated telomeres, compared to progenitor fibroblasts (Agarwal et al., 2010; Huang et al., 2011; Wang et al., 2012; Marion et al., 2009). Thus, it is not surprising that reduction of lamin A by shRNA also does not shorten the telomeres of iPS cells. Instead, lack of lamin A may facilitate telomere elongation in pluripotent stem cells. Lamina-associated domains represent a strongly repressive chromatin environment enriched by H3K9me2, H3K9me3 and H3K27me3, and restrict movement and expression of genes nearby (Guelen et al., 2008; Peric-Hupkes et al., 2010; Wen et al., 2009). Repressive lysine methylated histones negatively regulate telomere lengths likely by controlling telomere recombination (Benetti et al., 2007; Blasco, 2007). Sufficient telomere lengths are required to maintain chromosomal stability and pluripotency of ES/iPS cells (Huang et al., 2011). We extend the observations by generation of iPS cells, and further speculate that lamin A depletion in the nuclear envelope might facilitate movement of telomeres, accessible for telomere elongation associated proteins, as well as amenable for recombination to elongate telomeres, essential for maintenance of pluripotency of iPS/ES cells.

Manipulating lamin A levels may enhance reversal of aging by iPS technology

Successful generation and characterization of iPS cells from HGPS fibroblasts have been recently reported (Liu et al., 2011a; Liu et al., 2011b; Zhang et al., 2011). Remarkably, progerin expression and senescence phenotypes are lost in iPS cells but not in differentiated progeny. These new HGPS iPS cells are valuable for characterizing the role of progerin in driving HGPS and aging and for screening therapeutic strategies to prevent or delay cell senescence (Niedernhofer et al., 2011). A synergistic relationship between telomere dysfunction and progerin production may participate in the induction of cell senescence and normal aging process (Cao et al., 2011). Telomere length can be reset during induction of iPS from DKC patients (Agarwal and Daley, 2011). It would be interesting to know the telomere states during reprogramming to iPS cells from HGPS patients.

Together, levels of lamin A influence reprogramming and pluripotency. High levels of lamin A in differentiated cells or overexpression of lamin A retards iPS cell induction. On the contrary, lower levels of lamin A or depletion of lamin A by RNAi accelerate iPS cell formation. Human fibroblasts overexpressing lamin A exhibit accelerated telomere shortening and rapid replicative senescence and progroid phenotypes (Huang et al., 2008). Lamin A is involved in premature aging and also normal physiological aging (Kudlow and Kennedy, 2006; Scaffidi and Misteli, 2006). Generation of iPS cells by depletion of lamin A may enhance effectiveness in the processes of reversing cellular aging from older patients or premature aging patients and have implications in potential stem cell therapy.

Materials and Methods

Isolation of Mouse Embryonic Fibroblasts (MEF), adult Tail-Tip Fibroblasts (TTF) and Mesenchymal Stem Cells (MSC)

MEFs were derived from E13.5 embryos from C57BL/6J mice isolated by caesarean section and washed in HBSS. Heads and visceral tissues were removed, and remaining tissue was washed in fresh PBS, then submerged in 0.05 mM trypsin/1 mM EDTA HBSS solution and incubated at 37℃ for 10 min. Tissue was pipetted repeatedly to aid in tissue dissociation, then added to MEF media containing 10% FBS and plated (passage 0). Isolation of TTFs and MSCs was performed as described, respectively (Fan et al., 2011; Huang et al., 2011; Liu et al., 2004). The tails from adult mice were peeled, briefly rinsed with 70% ethanol, minced into 1×1 mm^3 pieces, placed onto culture dishes, and incubated for 7 days in MEF medium (DMEM containing 10% FBS). Cells that migrated out of the grafted pieces were transferred to new plates and maintained in MEF medium.

iPS cell induction

Derivation of iPS cells from TTFs or MEFs has been described previously (Huang et al., 2011; Wang et al., 2012). iPS cells were induced by transduction with four Yamanaka factors using standard protocol (Okita et al., 2007), with slight modification on induction media for some experiments. The day before transduction, Plat-E cells were seeded at 5×10^6 cells per 100 mm dish. On the next day, pMXs-based retroviral vectors (pMXs-Sox2, Klf4, Oct4, c-Myc) were introduced into Plat-E cells using lipo-2000 transfection reagent according to the manufacturer's recommendations. Infection cells were replated in 10 ml ES cell medium containing knock-out DMEM medium (Invitrogen), added with 20% FBS or 20% KSR, 1000 U/ml LIF, 0.1 mM β-mercaptoethanol, 1 mM L-glutamine and 0.1 mM non-essential amino acids, and antibiotics. Six days after infection, the cells were passaged on MEF feeders and the medium was changed every day. Twelve or 13 days after infection, ES-like colonies were picked and passaged using standard protocols. For alkaline phosphatase (AP) assay, 10,000 cells were plated in a 6-well plate, and the formed colonies assessed using the Vector blue kit from Vector Laboratories (USA).

ES cell culture

N33 ES cell lines as control were derived from C57BL/6J mice (Huang et al., 2011). The ES cell culture medium consisted of knock-out DMEM added with 15% (J1 ES) or 20% FBS (N33ES), 1000 U/ml leukemia inhibitory factor (LIF) (ESGRO, Chemicon), 0.1 mM non-essential amino acids, 0.1 mM β-mercaptoethanol, 1 mM L-glutamine, and penicillin (100 U/ml) and streptomycin (100 μg/ml). The medium was changed daily and cells were routinely passaged every 2 days.

Immunofluorescence microscopy

Immunofluorescence staining was performed as described (Huang et al., 2011). Cells were washed twice in phosphate buffered saline (PBS), then fixed in freshly

prepared 3.7% paraformaldehyde in PBS (pH 7.4), permeabilized in 0.1% Triton X-100 in blocking solution (3% goat serum in PBS) for 30 min, washed three times, and left in blocking solution for 1 h. Cells were incubated overnight at 4℃ with primary antibodies against Lamin A (Abcam, ab26300), Oct4 (sc5279, Santa Cruz, CA), Nanog (Abcam, ab10626), SSEA-1 (DSHB, MC-480), H3K4 (Abcam, ab1012), and H3K9 (Millipore, 07212), washed three times, and incubated for 2 h with secondary antibodies at RT, Alexa Fluor 488 goat anti-mouse (MP, A-11001), Alexa Fluor 568 goat anti-rabbit (MP, A-11011), diluted 1:200 with blocking solution. Samples were washed, and counterstained with 0.5 μg/ml Hochest33342 (MP, H1398) or DAPI in Vectashield mounting medium. Fluorescence was detected and imaged using a Leica inverted fluorescence microscope.

Western blot

Cells were washed twice in PBS, collected, and lysed in SDS Sample Buffer at 99℃ for 5 min; 25 μg total proteins of each cell extracts were resolved by 10–12% Bis-Tris SDS-PAGE and transferred to polyvinylidine difluoride membranes (PVDF, Millipore). Non-specific binding was blocked by overnight incubation in 5% skin milk in TBS at 4℃. Blots were then probed for 1–2 h at room temperature with anti-laminA (Rabbit polyclonal; Abcam, ab26300), anti-β-actin (Rabbit polyclonal; Santa Cruz, sc1616R). Immunoreactive bands were then probed for 1–2 h at room temperature with the appropriate horseradish peroxidase-conjugated secondary anti-Rabbit IgG -HRP (GE Healthcare 371624). Protein bands were detected by Enhanced ECL AmershamTM prime western blotting detection reagent (GE Healthcare RPN2232).

Quantitative real-time PCR

Total RNA was purified using a RNA mini kit (QIAGEN), treated with DNase I (Ambion), and the cDNA was generated from 0.2 μg RNA using random primers and SuperScript II (Invitrogen). Primers (supplementary material Table S1) were confirmed their specificity with dissociation curves. All data are normalized using β-actin as internal control. Quantitative real-time PCR was carried out on a MyiQ Detection system (BIO-RAD, USA) using SYBR Green I PCR Master Mix (TOYOBOL, JPN). For the analysis, all reactions (in triplicate) were carried out by amplifying target genes and endogenous controls in the same plate. The amplification was performed for primary denaturation at 95℃ for 1 min, then 40 cycles of denaturation at 95℃ for 15 s, annealing at 58℃ for 10 s and elongation at 72℃ for 15 s, and the last cycle under 55–95℃ for dissociation curve. Relative quantitative evaluation of target gene was determined by comparing the threshold cycles.

Generation of lamin A knockdown MEFs by shRNA

After initial test of four different shRNA designs against lamin A mRNA, the following shRNA sequence (19-nucleotide linker sense oligonucleotides, a hairpin loop, and an antisense of 19-nucleotide sense sequence, and an antisense of the linker) was used for the following experiment:

forward, GATCCGGAGCTTGACTTCCAGAAGTTCAAGAGACTTCTGGA-AGTCAAGCTCCTTTTTTAAGCTTG; reverse, AATTCAAGCTTAAAAAAG-GAGCTTGACTTCCAGAAGTCTCTTGAACTTCTGGAAGTCAAGCTCCG.

Control sequence:

forward, GATCCGGCGTTCAATTAGCAGACCATTCAAGAGATGGTCTG-CTAATTGAACGCCTTTTTTAAGCTTG; reverse, AATTCAAGCTTAAAAA-AGCGTTCAATTAGCAGACCATCTCTTGAATGGTCTGCTAATTGAACGCCG.

The shRNAs were cloned into pSITEN-RetroQ (Clontech), the resultant vector was transfected into Plat-E cells with lipofectamine 2000 according to the manufacturer's instruction to package, and corresponding retrovirus used to transfect C57BL/6 MEF as controls. C57BL/6 MEFs at same passages were transfected with lamin A shRNA and control shRNA virus enriched for 48 and 72 h, respectively. After each transfection with corresponding retrovirus, the media were changed to complete culture medium (ES media) at 8–12 h, and cells continued culture for 48 h, and were collected for immunostaining, western blot and real-time PCR analysis.

Telomere measurement by quantitative real-time PCR

Average telomere length was measured from total genomic DNA using a real-time PCR assay, as previously described (Cawthon, 2002), but modified for measurement of mouse telomeres (Callicott and Womack, 2006; Huang et al., 2011). Cells were washed in PBS and stored at −20℃ until subsequent DNA extraction. Genome DNA was prepared using DNeasy Blood & Tissue Kit (Qiagen, Valencia, CA). Average telomere length was measured from total genomic DNA using a real-time PCR assay, as previously described, but modified for measurement of mouse telomeres. PCR reactions were performed on the iCycler iQ real-time PCR detection system (Bio-Rad, Hercules, CA), using telomeric primers, primers for the reference control gene (mouse 36B4 single copy gene) and PCR settings as previously described. For each PCR reaction, a standard curve was made by serial dilutions of known amounts of DNA. The telomere signal was normalized to the signal from the single copy gene to generate a T/S ratio indicative of relative telomere length. Equal amounts of DNA (20 ng) were used for each reaction, with at least three replicates for each specimen.

Chromosome spreads and karyotyping

iPS cells were incubated with 0.5 μg/ml nocodazole for 1.5–2 h to arrest the cells in metaphase. The cells were exposed to hypotonic treatment with 75 mM KCl solution and fixed with methanol:glacial acetic acid (3:1) and spread onto clean slides.

Construction of lamin A overexpression vector

The full length 1666 bp *Lamina* was amplified from mouse ES cDNA using TransStar Fastpfu (Transgene) and cloned into pCMV-Tag2B. For lamin A overexpression in iPS induction experiments, cells at the concentration of 5×10^5 were transfected with the vectors using lipofectamine and 24 h later selected with 400 μg/ml G418 for 3 days. Samples were collected at 48 for analysis of efficiency of lamin A OE. Then, plates with the residual cells at 1×10^5 were used for iPS induction by the method using pMXs-Sox2, Klf4, Oct4, c-Myc described above, except for that 20% FBS was replaced by KSR in the media, and cells at 1×10^4 were plated on inactivated MEF feeders.

Fluorescent activated cell sorter (FACS) analysis

Flow cytometry analysis of the iPSCs were carried out using a BD LSR analyzer (BD Biosciences). The mean SSC-H was calculated by using CELLQuest Pro software. At least two independent pairs of Lmna knockdown or Lmna overexpression cells and controls were assayed to verify the percentage of GFP positive cells.

Statistical analysis

Percentages were transformed using arcsin transformation. Percentage transformed data and other number were analyzed by ANOVA and means compared by Fisher's protected least-significant difference (PLSD) using the StatView software from SAS Institute Inc. (Cary, NC). Linear relation analysis was performed using SigmaPlot 8.0. Significant differences were defined as $P<0.05$, 0.01 or lower.

Acknowledgements

We thank Minshu Li, Qian Zhang and Xiaoying Ye for help with the experiments. This work was supported by China MOST National Major Basic Research Program (2009CB941000, 2010CB94500). Author contributions: B.Z.: data collection, analysis and interpretation, manuscript writing; J.Y., F.W., L.W., Y.Y., J.D., N.L.: data collection and analysis. L.L.: conception and design, financial support, data interpretation, manuscript writing and final approval.

Competing Interests

The authors have no competing interests to declare.

References

Agarwal, S. and Daley, G. Q. (2011). Telomere dynamics in dyskeratosis congenita: the long and the short of iPS. *Cell Res.* **21**, 1157-1160.

Agarwal, S., Loh, Y. H., McLoughlin, E. M., Huang, J., Park, I. H., Miller, J. D., Huo, H., Okuka, M., Dos Reis, R. M., Loewer, S. et al. (2010). Telomere elongation in induced pluripotent stem cells from dyskeratosis congenita patients. *Nature* **464**, 292-296.

Andrés, V. and González, J. M. (2009). Role of A-type lamins in signaling, transcription, and chromatin organization. *J. Cell Biol.* **187**, 945-957.

Banito, A., Rashid, S. T., Acosta, J. C., Li, S., Pereira, C. F., Geti, I., Pinho, S., Silva, J. C., Azuara, V., Walsh, M. et al. (2009). Senescence impairs successful reprogramming to pluripotent stem cells. *Genes Dev.* **23**, 2134-2139.

Benetti, R., Gonzalo, S., Jaco, I., Schotta, G., Klatt, P., Jenuwein, T. and Blasco, M. A. (2007). Suv4-20h deficiency results in telomere elongation and derepression of telomere recombination. *J. Cell Biol.* **178**, 925-936.

Blasco, M. A. (2007). The epigenetic regulation of mammalian telomeres. *Nat. Rev. Genet.* **8**, 299-309.

Bridger, J. M. and Kill, I. R. (2004). Aging of Hutchinson-Gilford progeria syndrome fibroblasts is characterised by hyperproliferation and increased apoptosis. *Exp. Gerontol.* **39**, 717-724.

Broers, J. L., Ramaekers, F. C., Bonne, G., Yaou, R. B. and Hutchison, C. J. (2006). Nuclear lamins: laminopathies and their role in premature ageing. *Physiol. Rev.* **86**, 967-1008.

Bru, T., Clarke, C., McGrew, M. J., Sang, H. M., Wilmut, I. and Blow, J. J. (2008). Rapid induction of pluripotency genes after exposure of human somatic cells to mouse ES cell extracts. *Exp. Cell Res.* **314**, 2634-2642.

Burtner, C. R. and Kennedy, B. K. (2010). Progeria syndromes and ageing: what is the connection? *Nat. Rev. Mol. Cell Biol.* **11**, 567-578.

Butler, J. T., Hall, L. L., Smith, K. P. and Lawrence, J. B. (2009). Changing nuclear landscape and unique PML structures during early epigenetic transitions of human embryonic stem cells. *J. Cell. Biochem.* **107**, 609-621.
Callicott, R. J. and Womack, J. E. (2006). Real-time PCR assay for measurement of mouse telomeres. *Comp. Med.* **56**, 17-22.
Candelario, J., Sudhakar, S., Navarro, S., Reddy, S. and Comai, L. (2008). Perturbation of wild-type lamin A metabolism results in a progeroid phenotype. *Aging Cell* **7**, 355-367.
Cao, K., Blair, C. D., Faddah, D. A., Kieckhaefer, J. E., Olive, M., Erdos, M. R., Nabel, E. G. and Collins, F. S. (2011). Progerin and telomere dysfunction collaborate to trigger cellular senescence in normal human fibroblasts. *J. Clin. Invest.* **121**, 2833-2844.
Cawthon, R. M. (2002). Telomere measurement by quantitative PCR. *Nucleic Acids Res.* **30**, e47.
Chambers, I., Silva, J., Colby, D., Nichols, J., Nijmeijer, B., Robertson, M., Vrana, J., Jones, K., Grotewold, L. and Smith, A. (2007). Nanog safeguards pluripotency and mediates germline development. *Nature* **450**, 1230-1234.
Constantinescu, D., Gray, H. L., Sammak, P. J., Schatten, G. P. and Csoka, A. B. (2006). Lamin A/C expression is a marker of mouse and human embryonic stem cell differentiation. *Stem Cells* **24**, 177-185.
Csoka, A. B., English, S. B., Simkevich, C. P., Ginzinger, D. G., Butte, A. J., Schatten, G. P., Rothman, F. G. and Sedivy, J. M. (2004). Genome-scale expression profiling of Hutchinson-Gilford progeria syndrome reveals widespread transcriptional misregulation leading to mesodermal/mesenchymal defects and accelerated atherosclerosis. *Aging Cell* **3**, 235-243.
De Vos, W. H., Houben, F., Hoebe, R. A., Hennekam, R., van Engelen, B., Manders, E. M., Ramaekers, F. C., Broers, J. L. and Van Oostveldt, P. (2010). Increased plasticity of the nuclear envelope and hypermobility of telomeres due to the loss of A-type lamins. *Biochim. Biophys. Acta* **1800**, 448-458.
Dechat, T., Pfleghaar, K., Sengupta, K., Shimi, T., Shumaker, D. K., Solimando, L. and Goldman, R. D. (2008). Nuclear lamins: major factors in the structural organization and function of the nucleus and chromatin. *Genes Dev.* **22**, 832-853.
Decker, M. L., Chavez, E., Vulto, I. and Lansdorp, P. M. (2009). Telomere length in Hutchinson-Gilford progeria syndrome. *Mech. Ageing Dev.* **130**, 377-383.
Eminli, S., Foudi, A., Stadtfeld, M., Maherali, N., Ahfeldt, T., Mostoslavsky, G., Hock, H. and Hochedlinger, K. (2009). Differentiation stage determines potential of hematopoietic cells for reprogramming into induced pluripotent stem cells. *Nat. Genet.* **41**, 968-976.
Fan, G., Wen, L., Li, M., Li, C., Luo, B., Wang, F., Zhou, L. and Liu, L. (2011). Isolation of mouse mesenchymal stem cells with normal ploidy from bone marrows by reducing oxidative stress in combination with extracellular matrix. *BMC Cell Biol.* **12**, 30.
Gonzalez-Suarez, I., Redwood, A. B., Perkins, S. M., Vermolen, B., Lichtensztejin, D., Grotsky, D. A., Morgado-Palacin, L., Gapud, E. J., Sleckman, B. P., Sullivan, T. et al. (2009). Novel roles for A-type lamins in telomere biology and the DNA damage response pathway. *EMBO J.* **28**, 2414-2427.
Guelen, L., Pagie, L., Brasset, E., Meuleman, W., Faza, M. B., Talhout, W., Eussen, B. H., de Klein, A., Wessels, L., de Laat, W. et al. (2008). Domain organization of human chromosomes revealed by mapping of nuclear lamina interactions. *Nature* **453**, 948-951.
Ho, J. C., Zhou, T., Lai, W. H., Huang, Y., Chan, Y. C., Li, X., Wong, N. L., Li, Y., Au, K. W., Guo, D. et al. (2011). Generation of induced pluripotent stem cell lines from 3 distinct laminopathies bearing heterogeneous mutations in lamin A/C. *Aging (Albany NY)* **3**, 380-390.
Huang, S., Risques, R. A., Martin, G. M., Rabinovitch, P. S. and Oshima, J. (2008). Accelerated telomere shortening and replicative senescence in human fibroblasts overexpressing mutant and wild-type lamin A. *Exp. Cell Res.* **314**, 82-91.
Huang, J., Wang, F., Okuka, M., Liu, N., Ji, G., Ye, X., Zuo, B., Li, M., Liang, P., Ge, W. W. et al. (2011). Association of telomere length with authentic pluripotency of ES/iPS cells. *Cell Res.* **21**, 779-792.
Kudlow, B. A. and Kennedy, B. K. (2006). Aging: progeria and the lamin connection. *Curr. Biol.* **16**, R652-R654.
Lees-Miller, S. P. (2006). Dysfunction of lamin A triggers a DNA damage response and cellular senescence. *DNA Repair (Amst.)* **5**, 286-289.
Liu, L., DiGirolamo, C. M., Navarro, P. A., Blasco, M. A. and Keefe, D. L. (2004). Telomerase deficiency impairs differentiation of mesenchymal stem cells. *Exp. Cell Res.* **294**, 1-8.
Liu, G. H., Barkho, B. Z., Ruiz, S., Diep, D., Qu, J., Yang, S. L., Panopoulos, A. D., Suzuki, K., Kurian, L., Walsh, C. et al. (2011a). Recapitulation of premature ageing with iPSCs from Hutchinson-Gilford progeria syndrome. *Nature* **472**, 221-225.
Liu, G. H., Suzuki, K., Qu, J., Sancho-Martinez, I., Yi, F., Li, M., Kumar, S., Nivet, E., Kim, J., Soligalla, R. D. et al. (2011b). Targeted gene correction of laminopathy-associated LMNA mutations in patient-specific iPSCs. *Cell Stem Cell* **8**, 688-694.
Marion, R. M., Strati, K., Li, H., Tejera, A., Schoeftner, S., Ortega, S., Serrano, M. and Blasco, M. A. (2009). Telomeres acquire embryonic stem cell characteristics in induced pluripotent stem cells. *Cell Stem Cell* **4**, 141-154.
Mounkes, L. C., Kozlov, S., Hernandez, L., Sullivan, T. and Stewart, C. L. (2003). A progeroid syndrome in mice is caused by defects in A-type lamins. *Nature* **423**, 298-301.
Musich, P. R. and Zou, Y. (2009). Genomic instability and DNA damage responses in progeria arising from defective maturation of prelamin A. *Aging (Albany NY)* **1**, 28-37.
Naetar, N. and Foisner, R. (2009). Lamin complexes in the nuclear interior control progenitor cell proliferation and tissue homeostasis. *Cell Cycle* **8**, 1488-1493.
Niedernhofer, L. J., Glorioso, J. C. and Robbins, P. D. (2011). Dedifferentiation rescues senescence of progeria cells but only while pluripotent. *Stem Cell Res Ther* **2**, 28.
Niwa, H., Miyazaki, J. and Smith, A. G. (2000). Quantitative expression of Oct-3/4 defines differentiation, dedifferentiation or self-renewal of ES cells. *Nat. Genet.* **24**, 372-376.
Okada, M., Oka, M. and Yoneda, Y. (2010). Effective culture conditions for the induction of pluripotent stem cells. *Biochim. Biophys. Acta* **1800**, 956-963.
Okita, K., Ichisaka, T. and Yamanaka, S. (2007). Generation of germline-competent induced pluripotent stem cells. *Nature* **448**, 313-317.
Pekovic, V. and Hutchison, C. J. (2008). Adult stem cell maintenance and tissue regeneration in the ageing context: the role for A-type lamins as intrinsic modulators of ageing in adult stem cells and their niches. *J. Anat.* **213**, 5-25.
Peric-Hupkes, D., Meuleman, W., Pagie, L., Bruggeman, S. W., Solovei, I., Brugman, W., Gräf, S., Flicek, P., Kerkhoven, R. M., van Lohuizen, M. et al. (2010). Molecular maps of the reorganization of genome-nuclear lamina interactions during differentiation. *Mol. Cell* **38**, 603-613.
Röber, R. A., Weber, K. and Osborn, M. (1989). Differential timing of nuclear lamin A/C expression in the various organs of the mouse embryo and the young animal: a developmental study. *Development* **105**, 365-378.
Rodriguez, S., Coppedè, F., Sagelius, H. and Eriksson, M. (2009). Increased expression of the Hutchinson-Gilford progeria syndrome truncated lamin A transcript during cell aging. *Eur. J. Hum. Genet.* **17**, 928-937.
Scaffidi, P. and Misteli, T. (2006). Lamin A-dependent nuclear defects in human aging. *Science* **312**, 1059-1063.
Scaffidi, P. and Misteli, T. (2008). Lamin A-dependent misregulation of adult stem cells associated with accelerated ageing. *Nat. Cell Biol.* **10**, 452-459.
Shimi, T., Pfleghaar, K., Kojima, S., Pack, C. G., Solovei, I., Goldman, A. E., Adam, S. A., Shumaker, D. K., Kinjo, M., Cremer, T. et al. (2008). The A- and B-type nuclear lamin networks: microdomains involved in chromatin organization and transcription. *Genes Dev.* **22**, 3409-3421.
Stewart, C. and Burke, B. (1987). Teratocarcinoma stem cells and early mouse embryos contain only a single major lamin polypeptide closely resembling lamin B. *Cell* **51**, 383-392.
Sullivan, T., Escalante-Alcalde, D., Bhatt, H., Anver, M., Bhat, N., Nagashima, K., Stewart, C. L. and Burke, B. (1999). Loss of A-type lamin expression compromises nuclear envelope integrity leading to muscular dystrophy. *J. Cell Biol.* **147**, 913-920.
Takamori, Y., Tamura, Y., Kataoka, Y., Cui, Y., Seo, S., Kanazawa, T., Kurokawa, K. and Yamada, H. (2007). Differential expression of nuclear lamin, the major component of nuclear lamina, during neurogenesis in two germinal regions of adult rat brain. *Eur. J. Neurosci.* **25**, 1653-1662.
Uhlírová, R., Horáková, A. H., Galiová, G., Legartová, S., Matula, P., Fojtová, M., Varecha, M., Amrichová, J., Vondrácek, J., Kozubek, S. et al. (2010). SUV39h- and A-type lamin-dependent telomere nuclear rearrangement. *J. Cell. Biochem.* **109**, 915-926.
Wang, F., Yin, Y., Ye, X., Liu, K., Zhu, H., Wang, L., Chiourea, M., Okuka, M., Ji, G., Dan, J. et al. (2012). Molecular insights into the heterogeneity of telomere reprogramming in induced pluripotent stem cells. *Cell Res.* **22**, 757-768.
Wen, B., Wu, H., Shinkai, Y., Irizarry, R. A. and Feinberg, A. P. (2009). Large histone H3 lysine 9 dimethylated chromatin blocks distinguish differentiated from embryonic stem cells. *Nat. Genet.* **41**, 246-250.
Zhang, J., Lian, Q., Zhu, G., Zhou, F., Sui, L., Tan, C., Mutalif, R. A., Navasankari, R., Zhang, Y., Tse, H. F. et al. (2011). A human iPSC model of Hutchinson Gilford Progeria reveals vascular smooth muscle and mesenchymal stem cell defects. *Cell Stem Cell* **8**, 31-45.